

# Studying the squeezing effect and phase space distribution of single- photon- added coherent state using postselected von Neumann measurement

Wen Jun Xu, Taximaiti Yusufu and Yusuf Turek\*

*School of Physics and Electronic Engineering, Xinjiang Normal University, Urumqi, Xinjiang 830054, China*

(Dated: November 19, 2021)

In this paper, ordinary and amplitude-squared squeezing as well as Winger function of single-photon-added coherent state after postselected von Neumann measurement are investigated. The analytical results showed that the von Neumann type measurement which characterized by postselection and weak value could change the squeezing feature of single-photon-added coherent state significantly. It is also investigated that the postselected measurement can increase the nonclassicality of the original state in strong measurement regimes. It anticipated that this work could provide other effective methods to the related state optimization problems based on the postselected von Neumann measurement technique.

PACS numbers: xxxxx

## I. INTRODUCTION

The states possess nonclassical features are important resources for quantum information processing and investigating fundamental problems of quantum theory. It showed that the squeezed states of radiation field has been considered as a truly quantum [1]. In recent years the studies about the squeezing especially the quadrature squeezing of the radiation fields has been payed great attention since it has have many applicaitons in optical communication and information theory [2–13], gravitatioanl wave detection [14], quantum teleportation [14–22], dense coding [23], resonance fluorescence [24], and quantum cryptography [25]. Furthermore, with the rapid development of the techniques for making higher-order correlation measurements in quantum optics and laser physics, the high-order squeezing effect of radiation field also became the hot topic in sate optimization researches. The higher-order squeezing of radiation field firstly introduced by Hong and Manel [26] in 1985, and Hiley [27, 28] defined another type higher-order squeezing, named amplitude- squared squeezing (ASS) of the electromagnetic field in 1987. After that the higher squeezing of radiation fields has been investigated in many research fields [29–45].

We know that the squeezing is an inherent feature of nonclassical states, and its improvement requires take optimization on it. Some states initially not possess squeezing, but after taking the optimization process it repossess the pronounced squeezing effect, i.e., the single-photon-added coherent state (SPACS) is a typical example. SPACAS is created by adding the creation operator  $a^\dagger$  to the coherent state, and this optimization changed the coherent state from semi-classical to new quantum state which possess squeezing. Since this state have wide applications in many quantum information processing including entanglement state generation[], quantum

key distribution [46, 47], and quantum digital signature [48], the optimization for this state is worthy to study for provide other new effective methods to the implementations of related processes. On the other hand, the weak signal amplification technique proposed in 1988 [49] by Aharonov, Albert, and Vaidman widely used in state optimization and precision measurement problems [50–56]. Most recently, one of the authors of this paper investigated the effects of postselected von Neumann measurement on the properties of single-mode radiation fields [55, 56] and found that postselected von Neumann measurement really changed the photon statistics and quadrature squeezing of radiation fields for different anomalous weak values and coupling strengths. However, to our knowledge, the effects of postselected von Neumann measurement on higher-order squeezing and phase space distribution of SPACS have not been previously investigated yet.

In this work, motivated by our previous works [53, 55, 56], we study the squeezing and Winger function of SPACS after postselected von Neumann measurement. In this work, we take the spatial and polarization degrees of freedom of SPACS as measuring device (pointer) and system, respectively, and consider all orders of time evolution operator. After getting the final state of the pointer, we check the criteria of existence of squeezing of SPACS, and found that the postselected measurement has positive effects to the squeezing of SPACS in weak measurement regime. Furthermore, we investigate the state distance and the Wigner function of the SPACS after measurement. We found that with increasing the coupling strength the original SPACS spoiled significantly, and the state gets more pronounced negative areas as well as interference structures in phase space after postselected measurement. In a word, we observed that the postselected von Neumann measurement really has positive effects to its nonclassicality including squeezing effects especially in weak measurement regime. These results can be considered as a result of weak value amplification of weak measurement technique.

The rest of the paper is organized as follows. In Sec.

\* [yusufturek@xjnu.edu.cn](mailto:yusufturek@xjnu.edu.cn)

**II**, we introduce the main concepts of our scheme and derive the final pointer state after postselected measurement which will be used throughout the study. In Sec. **III**, we give the details of ordinary squeezing and ASS effects of final pointer state. In Sec. **IV**, we investigate the state distance and the Wigner function SPACS after measurement. We give a conclusion to our paper in Sec. **V**.

## II. MODEL AND THEORY

In this part, we introduce the basic concepts of postselected von Neumann measurement and give the expression of final pointer state which we used in this paper. We know that the every measurement problems consists three main parts such as pointer(measuring device), measured system and environment. In current work, we take that the spatial and polarization degrees of freedom of SPACS as pointer and system, respectively. In general, in measurement problems we want to get the interested system information by comparing the state shifts of the pointer after measurement finished, and do not consider the spoiling of the pointer in entire measurement process. Here, contrary to the standard goal of the measurement, we investigate the effects of pre- and post-selected measurement taken on beam's polarization(measured system) on the inherent properties of beam's spatial part (pointer). Since in measurement process the system and pointer Hamiltonians does not effect the final read outs, it is enough to us only consider the interaction Hamiltonian of them to begin our purposes. According to the standard von Neumann measurement theory, the interaction Hamiltonian between the system and the pointer takes as [57]

$$\hat{H} = g(t)\hat{A} \otimes \hat{P}. \quad (1)$$

Here,  $\hat{A}$  is system observable we want to measure, and  $\hat{P}$  is the momentum operator of the pointer conjugated to the position operator,  $[\hat{X}, \hat{P}] = i$ .  $g(t)$  is coupling strength function between system and pointer and it assumed exponentially small except during a period of interaction time of order  $T$ , and normalized according to  $\int_{-\infty}^{+\infty} g(t)dt = \int_0^T g(t)dt = g_0$ . In this work, assume that the system observable  $\hat{A}$  is Pauli  $x$  matrix, i.e.,

$$\hat{A} = \hat{\sigma}_x = |H\rangle\langle V| + |V\rangle\langle H| = \begin{pmatrix} 0 & 1 \\ 1 & 0 \end{pmatrix} \quad (2)$$

Here,  $|H\rangle \equiv (1, 0)^T$  and  $|V\rangle \equiv (0, 1)^T$  are represents the horizontal and vertical polarization of the beam, respectively. We also assume that in our scheme the pointer and measured system initially prepared to

$$|\phi\rangle = \gamma a^\dagger |\alpha\rangle, \quad \gamma = \frac{1}{\sqrt{1 + |\alpha|^2}} \quad (3)$$

and

$$|\psi_i\rangle = \cos \frac{\varphi}{2} |H\rangle + e^{i\delta} \sin \frac{\varphi}{2} |V\rangle, \quad (4)$$

respectively. Here,  $\alpha = re^{i\theta}$  and  $\delta \in [0, 2\pi]$  and  $\varphi \in [0, \pi]$ . Here, we have remind that in weak measurement theory the interaction strength between the system and measuring is too weak, and it is enough only to consider the evolution of unitary operator up to its first order. However, if we want to connect the weak and strong measurement and investigate the measurement feedback of postselected weak measurement, and analyze experimental results obtained in nonideal measurements, the full-order evolution of unitary operator is needed [58–60], and we call this kind of measurement is postselected von Neumann measurement. Thus, the evolution operator of this total system corresponding to the interaction Hamiltonian, Eq. (1), is evaluated as

$$e^{-ig_0\sigma_x \otimes P} = \frac{1}{2} \left( \hat{I} + \hat{\sigma}_x \right) \otimes D\left(\frac{s}{2}\right) + \frac{1}{2} \left( \hat{I} - \hat{\sigma}_x \right) \otimes D\left(-\frac{s}{2}\right) \quad (5)$$

since  $\hat{\sigma}_x^2 = 1$ . Here, we  $s = \frac{g_0}{\sigma}$  is the ratio between the coupling strength and beam width, and it can characterize the measurement types, i.e, the measurement is called weak measurement (strong measurement) if  $s < 1$  ( $s > 1$ ).  $D(\frac{s}{2})$  is the displacement operator defined as  $D(\alpha) = e^{\alpha\hat{a}^\dagger - \alpha^*\hat{a}}$ . We have to mention that the results of our current research are valid for weak and strong measurement regimes since we take into account the all orders of time evolution operator, Eq. (5). In above calculation we use the definition of momentum operator represented in Fock space in terms of annihilation (creation) operator  $\hat{a}$  ( $\hat{a}^\dagger$ ), i.g.,

$$\hat{P} = \frac{i}{2\sigma} (a^\dagger - a) \quad (6)$$

where  $\sigma$  width of the beam. Thus, the total state of the system,  $|\psi_i\rangle \otimes |\phi\rangle$ , after the time evolution becomes as

$$|\Psi\rangle = e^{-ig_0\sigma_x \otimes P} |\psi_i\rangle \otimes |\phi\rangle = \frac{1}{2} \left[ \left( \hat{I} + \hat{\sigma}_x \right) \otimes D\left(\frac{s}{2}\right) + \left( \hat{I} - \hat{\sigma}_x \right) \otimes D\left(-\frac{s}{2}\right) \right] |\psi_i\rangle \otimes |\phi\rangle \quad (7)$$

After we take strong projective measurement to the polarization degree of the beam with postselected state  $|\psi_f\rangle = |H\rangle$ , the above evolutioned total system state give us the final state of the pointer, and its normalized expression reads as

$$|\Phi\rangle = \frac{\kappa}{\sqrt{2}} \left[ (1 + \langle \sigma_x \rangle_w) D\left(\frac{s}{2}\right) + (1 - \langle \sigma_x \rangle_w) D\left(-\frac{s}{2}\right) \right] |\phi\rangle. \quad (8)$$

Here,

$$\kappa^{-2} = 1 + |\langle \sigma_x \rangle|^2 + \gamma^2 e^{-\frac{s^2}{2}} \text{Re}[(1 + \langle \sigma_x \rangle_w^*) (1 - \langle \sigma_x \rangle_w) \times (\gamma^{-2} - s^2 + \alpha s - \alpha^* s) e^{2s i \Im(\alpha)}] \quad (9)$$

is the normalization coefficient, and the weak value of the system observable  $\hat{\sigma}_x$  is given by

$$\langle \sigma_x \rangle_w = \frac{\langle \psi_f | \sigma_x | \psi_i \rangle}{\langle \psi_f | \psi_i \rangle} = e^{i\delta} \tan \frac{\varphi}{2}. \quad (10)$$

In general, the expectation value of  $\sigma_x$  is bounded  $-1 \leq \langle \sigma_x \rangle \leq 1$  for any associated system state. However, as we seen in Eq. (10), the weak values of the observable  $\sigma_x$  can take arbitrary large numbers with small successful post-selection probabilities  $P_s = |\langle \psi_f | \psi_i \rangle|^2 = \cos^2 \frac{\varphi}{2}$ . This feature of weak value is used to amplify very weak but useful information of various of related physical systems.

The state given in Eq. (8) is spoiled version of SPACS after postselected measurement. In next sections, we study its squeezing effects, and nonclassicality features characterized by Wigner function.

### III. ORDINARY AND AMPLITUDE SQUARE SQUEEZING

In this section, we check the ordinary (first-order) and ASS (second order) squeezing effects of SPACS after postselected von Neumann measurement. The squeezing effect is one of the non-classical phenomena unique to the quantum light field. The squeezing reflects the non-classical statistical properties of the optical field by a noise component lower than that of the coherent state. In other words, the noise of an orthogonal component of the squeezed light is lower than the noise of the corresponding component of the coherent state light field. In practice, if this component is used to transmit information, a higher signal-to-noise ratio can be obtained than that of the coherent state. Consider a single mode of electromagnetic field of frequency  $\omega$  with creation and annihilation operator  $a^\dagger, a$ . The quadrature and square of the field mode amplitude can be defined by operators

$X_\theta$  and  $Y_\theta$  as [61]

$$X_\theta \equiv \frac{1}{2} (ae^{-i\theta} + a^\dagger e^{i\theta}) \quad (11)$$

and

$$Y_\theta \equiv \frac{1}{2} (a^2 e^{-i\theta} + a^{\dagger 2} e^{i\theta}), \quad (12)$$

respectively. For these operators, if  $\Delta X_\theta \equiv X_\theta - \langle X_\theta \rangle$ ,  $\Delta Y_\theta \equiv Y_\theta - \langle Y_\theta \rangle$ , the minimum variances are seen to be [62]

$$\langle (\Delta X_\theta)^2 \rangle_{min} = \frac{1}{4} + \frac{1}{2} [(\langle a^\dagger a \rangle - |\langle a \rangle|^2) - (|\langle a^2 \rangle - \langle a \rangle^2|)] \quad (13)$$

$$\begin{aligned} \langle (\Delta Y_\theta)^2 \rangle_{min} &= \langle a^\dagger a + \frac{1}{2} \rangle \\ &+ \frac{1}{2} [\langle a^{\dagger 2} a^2 \rangle - |\langle a^2 \rangle|^2 - |\langle a^4 \rangle - \langle a^2 \rangle^2|] \end{aligned} \quad (14)$$

where  $a$  and  $a^\dagger$  are annihilation and creation operators of radiation field. If  $\langle (\Delta X_\theta)^2 \rangle_{min} < \frac{1}{4}$ ,  $X_\theta$  is said to be ordinary squeezed and if  $\langle (\Delta Y_\theta)^2 \rangle_{min} < \langle a^\dagger a + \frac{1}{2} \rangle$ ,  $Y_\theta$  is said to be ASS. These conditions can be rewritten as

$$S_{os} = \langle a^\dagger a \rangle - |\langle a \rangle|^2 - |\langle a^2 \rangle - \langle a \rangle^2| < 0 \quad (15)$$

$$S_{ass} = \langle a^{\dagger 2} a^2 \rangle - |\langle a^2 \rangle|^2 - |\langle a^4 \rangle - \langle a^2 \rangle^2| < 0. \quad (16)$$

Thus, the system characterized by any wave function could exhibit non-classical features if it satisfies Eqs. (15-16). To get our goal, first of all we have to calculate the above related quantities and their explicit expressions under the state  $|\Phi\rangle$  are listed below.

1. The expectation value  $\langle a^\dagger a \rangle$  under the state  $|\Psi\rangle$  is given by

$$\langle a^\dagger a \rangle = |\kappa|^2 \{ |1 + \langle \sigma_x \rangle_w|^2 t_1(s) + |1 - \langle \sigma_x \rangle_w|^2 t_1(-s) + 2Re[(1 - \langle \sigma_x \rangle_w)(1 + \langle \sigma_x \rangle_w)^* t_3(s)] \} \quad (17)$$

where

$$t_1(s) = \gamma^2 ((2 + |\alpha|^4 + s|\alpha|^2) Re(\alpha) + 3\alpha\alpha^* + 1) + \frac{s^2}{4}$$

and

$$\begin{aligned} t_3(s) &= \frac{1}{4} \gamma^2 e^{2isIm(\alpha)} e^{-\frac{s^2}{2}} (4|\alpha|^4 - 6s\alpha|\alpha|^2 + 2(6\alpha\alpha^* + s\alpha^{*2}(3\alpha + s) \\ &+ sRe(\alpha)(8 - 9s\alpha - 3s^2)) + 11\alpha^2 s^2 + s^4 + 6\alpha s^3 - 5s^2 - 16\alpha s + 4) \end{aligned}$$

respectively.

2. The expectation value  $\langle a \rangle$  under the state  $|\Psi\rangle$  is given by

$$\begin{aligned}\langle a \rangle &= |\kappa|^2 \gamma^2 \{ |1 + \langle \sigma_x \rangle_w|^2 \left[ 2\alpha + \alpha|\alpha|^2 + \frac{s}{2\gamma^2} \right] + |1 - \langle \sigma_x \rangle_w|^2 \left[ 2\alpha + \alpha|\alpha|^2 - \frac{s}{2\gamma^2} \right] \\ &\quad + (1 - \langle \sigma_x \rangle_w) (1 + \langle \sigma_x \rangle_w)^* w_1(s) + (1 + \langle \sigma_x \rangle_w) (1 - \langle \sigma_x \rangle_w)^* w_1(-s) \} \end{aligned}\quad (18)$$

where

$$w_1(s) = \frac{1}{2} e^{2isIm(\alpha)} e^{-\frac{s^2}{2}} (4\alpha + \alpha^*(s - 2\alpha)(s - \alpha) + 2\alpha^2 s + s^3 - 3\alpha s^2 - 3s)$$

3. The expectation value  $\langle a^2 \rangle$  under the state  $|\Psi\rangle$  is given by

$$\begin{aligned}\langle a^2 \rangle &= |\kappa|^2 \{ |1 + \langle \sigma_x \rangle_w|^2 q_1(s) + |1 - \langle \sigma_x \rangle_w|^2 q_1(-s) + (1 - \langle \sigma_x \rangle_w) (1 + \langle \sigma_x \rangle_w)^* q_2(s) \\ &\quad + (1 + \langle \sigma_x \rangle_w) (1 - \langle \sigma_x \rangle_w)^* q_2(-s) \} \end{aligned}\quad (19)$$

where

$$q_1(s) = \frac{1}{4} \gamma^2 (2\alpha + s)(6\alpha + |\alpha|^2(2\alpha + s) + s)$$

and

$$q_2(s) = -\frac{1}{4} e^{2isIm(\alpha)} e^{-\frac{s^2}{2}} \gamma^2 (s - 2\alpha)(6\alpha + \alpha^*(s - 2\alpha)(s - \alpha) + 2\alpha^2 s + s^3 - 3\alpha s^2 - 5s)$$

respectively.

4. The expectation value  $\langle a^{\dagger 2} a^2 \rangle$  under the state  $|\Psi\rangle$  is given by

$$\langle a^{\dagger 2} a^2 \rangle = |\kappa|^2 \{ |1 + \langle \sigma_x \rangle_w|^2 f_1(s) + |1 - \langle \sigma_x \rangle_w|^2 f_2(-s) + 2Re[(1 - \langle \sigma_x \rangle_w) (1 + \langle \sigma_x \rangle_w)^* f_3(s)] \} \quad (20)$$

where

$$\begin{aligned}f_1(s) &= \frac{1}{2} \gamma^2 (2|\alpha|^6 + s|\alpha|^2((s^2 + 16)Re(\alpha) + sRe(\alpha^2)) + 2|\alpha|^4(2sRe(\alpha) + s^2 + 5) \\ &\quad + 8\alpha^*\alpha + 6s^2\alpha^*\alpha + (2s^3 + 8s)Re(\alpha) + 3s^2Re(\alpha^2)) + \frac{s^4}{16} + \gamma^2 s^2\end{aligned}$$

and

$$\begin{aligned}f_3(s) &= -\frac{1}{16} \gamma^2 (s - 2\alpha)(2\alpha^* + s) \\ &\quad (2(\alpha^*)^2(s - 2\alpha)(s - \alpha) + 20|\alpha|^2 + 3s\alpha^*(s - 2\alpha)(s - \alpha) + 28isIm(\alpha) + s^2(2\alpha^2 + s^2 - 3\alpha s - 9) + 16e^{-\frac{1}{2}s(s - 4iIm[\alpha])})\end{aligned}$$

respectively.

5. The expectation value  $\langle a^4 \rangle$  under the state  $|\Psi\rangle$  is given by

$$\langle a^4 \rangle = |\kappa|^2 \{ |1 + \langle \sigma_x \rangle_w|^2 h_1(s) + |1 - \langle \sigma_x \rangle_w|^2 h_1(-s) + (1 + \langle \sigma_x \rangle_w)^* (1 - \langle \sigma_x \rangle_w) h_2(s) \} \quad (21)$$

$$+ (1 + \langle \sigma_x \rangle_w) (1 - \langle \sigma_x \rangle_w)^* h_2(-s) \quad (22)$$

where

$$h_1(s) = \frac{1}{16} (8\alpha\gamma^2|\alpha|^2(\alpha + s)(2\alpha^2 + s^2 + 2\alpha s) + s^4 + 8\alpha\gamma^2(10\alpha^3 + 2s^3 + 9\alpha s^2 + 16\alpha^2 s))$$

and

$$h_2(s) = -\frac{1}{16} \gamma^2 e^{2isIm(\alpha)} e^{-\frac{s^2}{2}} (s - 2\alpha)^3 (10\alpha + \alpha^*(s - 2\alpha)(s - \alpha) + 2\alpha^2 s + s^3 - 3\alpha s^2 - 9s)$$

respectively.

According to the expression of  $S_{os}$ , the curves for this quantity are plotted, and the analytical results are

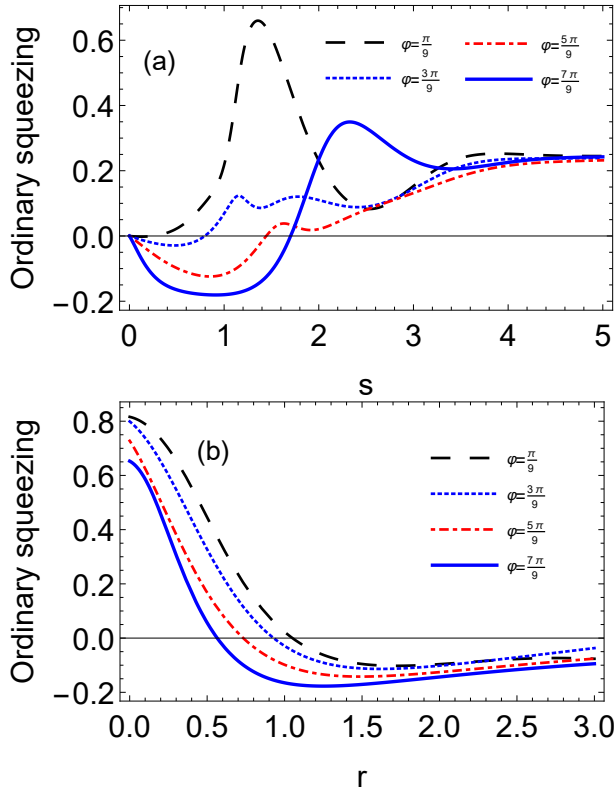


Figure 1. (Color online) The effects of postselected von Neumann measurement on ordinary squeezing of SPACS. Fig. 1(a) show the quantity  $S_{os}$  as a function of coupling strength for different weak values with fixed coherent state parameter ( $r = 1$ ). Fig. 1(b) show quantity  $S_{os}$  as a function of coherent state parameter  $r$  for different weak values with fixed coupling strength ( $s = 0.5$ ). Here, we take  $\theta = \frac{\pi}{4}$ ,  $\delta = \frac{\pi}{6}$ .

showed in Fig. 1. In Fig. 1(a), we fixed the parameter to  $r = 1$  and plot the  $S_{os}$  as a function of coupling strength  $s$  for different weak values quantified by  $\varphi$ . As we observed, when there is no interaction between system and pointer ( $s = 0$ ), there is no ordinary squeezing effect of initial SPACS at  $r = 1$  point. However, in moderate coupling strengths region such as  $0 < s < 2$ , the ordinary squeezing effect of SPACS is proportional to the weak value, i.e., the larger the weak value, the better its squeezing effect. From Fig. 1(a) we also can see that the ordinary squeezing effect of the light field gradually disappeared and tended to the same value for different weak values with increasing the coupling strength  $s$  in strong measurement regime. In Fig. 1(b), we plot the  $S_{os}$  as a function of state parameter  $r$  in weak measurement regime by fixing the coupling strength  $s$ , i.g.,  $s = 0.5$ . It is very clear from those curves presented in Fig. 1 (b) that the ordinary squeezing effect of SPACS is increased with increasing the weak value, especially when  $\varphi$  taken  $\frac{7\pi}{9}$ . Furthermore, along with the increases of  $r$  (after the  $r$  value exceed 1.5), the squeezing effect of the field for different weak values tended to be the same. According to the von Neumann measurement theory, when the inter-

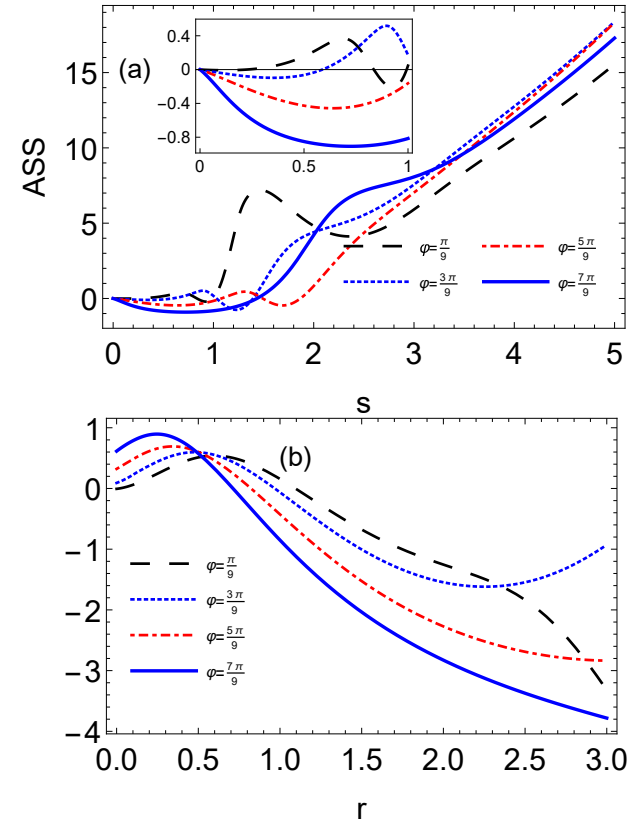


Figure 2. (Color online) The effects of postselected von Neumann measurement on ASS of SPACS. (a) the  $S_{ass}$  as a function of coupling strength  $s$  for different weak values with fixed coherent stat parameter  $r$  ( $r = 1$ ); (b) the  $S_{ass}$  as a function of coherent state parameter  $r$  for different weak values with fixed weak coupling strength  $s$  ( $s = 0.5$ ). Other parameters are the same as Fig. (1).

action strength is too large, the system is strongly measured and the size of the weak value has little effect on the squeezing effect[Ref]. This statement also can be observed in Fig. 1(a) and (b). In a word, in weak measurement regime the SPACS showed good ordinary squeezing effect after postselected measurement with large weak values, and it can be seen as a result of signal amplification feature of weak measurement technique.

The quantity  $S_{ass}$  can characterize the ASS of SPACS if it takes negative value, and in Fig. 2 it is plotted as a function of various system parameters. As indicated in Fig. 2 (a), when we fixed the coherent state parameter  $r$  the  $S_{ass}$  can take negative value in weak measurement regime ( $s < 1$ ) and its negativity increased as increasing the weak value quantified by  $\varphi$ . That is to say, in weak measurement regime the magnitude of the weak value has a linear relationship with the ASS effect of SPACS, i.g., the larger the weak value, the better the ASS effect. However, with increasing the coupling strength the value of  $S_{ass}$  became larger than zero and it indicated that there is no ASS effect of SPACS in postselected strong measurement regime ( $s > 1$ ) no matter how large the

weak value is taken. In order to further investigate the ASS of the radiation field in weak measurement regime, we plot the  $S_{ass}$  as a function of coherent state parameter  $r$  for different weak values with take  $s = 0.5$ , and its analytical results showed in Fig. 2(b). We can see that when  $r$  is relatively small, there is ASS effect no matter how large the weak value is taken. But as increasing the system parameter  $r$ , the  $S_{ass}$  become takes negative values and its negativity proportional to  $r$ . From the Fig. 2(a) we also can observe that in weak measurement regime the weak value really have positive effects to the ASS of SPACS, and it can also be considered as a result of weak signal amplification feature of postselected weak measurement technique.

#### IV. STATE DISTANCE AND WIGNER FUNCTION

The postselected measurement taken on polarization degree freedom of the beam could spoil the inherent properties presented in its spatial part. Before investigate the phase space distribution of SPACS after postselected von Neumann measurement, we check the similarity between the initial SPACS  $|\phi\rangle$  and the state  $|\Phi\rangle$  after measurement. The state distance between those two states can be evaluated by

$$F = |\langle\phi|\Phi\rangle|^2, \quad (23)$$

and its value is bounded  $0 \leq F \leq 1$ . If  $F = 1$  ( $F = 0$ ), then the two states are totally same (totally different). The  $F$  for our case can be calculated after substituting the Eq. (3) and Eq. (8) into the Eq. (23), and its analytical results showed in Fig. 3. In Fig. 3 we presented the state distance  $F$  as a function of system parameter  $r$  for different coupling strengths with a fixed large weak value. As shown in Fig. 3, in weak coupling regime ( $s = 0.5$ ), the state after postselected measurement is keep its similarity with coherent state parameter  $r$ . However, with increasing the measurement strength the initial state  $|\phi\rangle$  is spoiled and the similarity between the pointer states before and after measurement is decreased.

In order to further explain the squeezing effects of SPACS after postselected von Neumann measurement, in the rest of this section we study the Wigner function of the  $|\Phi\rangle$ . The Wigner distribution function is the closest quantum analogue of the classical distribution function in the phase space. According to the value of the Wigner function we can intuitively determine the strength of its quantum nature, and the negative value of the Wigner function proves the nonclassicality of the quantum state. The Wigner function is exist for any state, it is defined as the two-dimensional Fourier transform of the symmetric order characteristic function. Thus, the wigner function for the state  $\rho = |\Phi\rangle\langle\Phi|$  is written as [61]

$$W(z) \equiv \frac{1}{\pi^2} \int_{-\infty}^{+\infty} \exp(\lambda^* z - \lambda z^*) C_W(\lambda) d^2 \lambda, \quad (24)$$

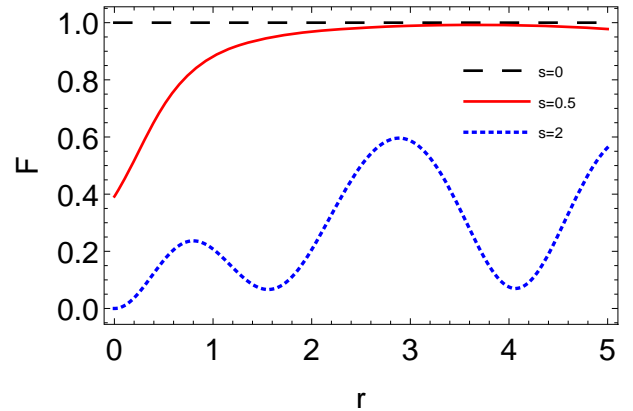


Figure 3. (Color online) The state distance between  $|\Phi\rangle$  and initial SPACS  $|\phi\rangle$  as a function of coherent state parameter  $r$  for various coupling strengths. Here, we take  $\theta = \frac{\pi}{4}$ ,  $\delta = \frac{\pi}{6}$ ,  $\varphi = \frac{7\pi}{9}$ .

where  $C_N(\lambda)$  is the normal ordered characteristic function, and defined as

$$C_W(\lambda) = \text{Tr} \left[ \rho e^{\lambda a^\dagger - \lambda^* a} \right]. \quad (25)$$

Using the notation  $\lambda', \lambda''$  for the real and imaginary parts of  $\lambda$  and setting  $z = x + ip$  to emphasize the analogy between the radiation field quadratures and normalized dimensionless position and momentum observables of the beam in phase space. We can rewrite the definition of Wigner function in terms of  $x, p$  and  $\lambda', \lambda''$  as

$$W(x, p) = \frac{1}{\pi^2} \int_{-\infty}^{+\infty} e^{2i(p\lambda' - x\lambda'')} C_W(\lambda) d\lambda' d\lambda''. \quad (26)$$

By substituting the final normalized pointer state  $|\Phi\rangle$  into Eq. (26), we can calculate the explicit expression of its Wigner function and it reads as

$$\begin{aligned} W(z) = & \frac{2|\kappa|^2}{\pi(1+|\alpha|^2)} e^{-2|z-\alpha|^2} \times \\ & \{ |1 + \langle\sigma_x\rangle_w|^2 w(\Gamma) + |1 - \langle\sigma_x\rangle_w|^2 w(-\Gamma) \\ & + 2(-1 + |2z - \alpha|^2) \text{Re}[(1 + \langle\sigma_x\rangle_w)^*(1 - \langle\sigma_x\rangle_w) e^{2isIm[z]}] \}. \end{aligned} \quad (27)$$

with

$$\begin{aligned} w(\Gamma) = & e^{-\frac{1}{2}s^2} e^{-2(\text{Re}[\alpha] - \text{Re}[z])s} \times \\ & \left( -1 + |2z - \alpha|^2 + 2s(\text{Re}[\alpha] - 2\text{Re}[z] + \frac{s}{2}) \right) \end{aligned} \quad (28)$$

This is a real Wigner function and its vale is bounded  $-\frac{2}{\pi} \leq W(\alpha) \leq \frac{2}{\pi}$  in whole phase space.

To depict the effects of the postselected von Neumann measurement on the non-classical feature of SPACS, in Fig. 4 we plot its curves for different parametric coherent state parameters  $r$  and coupling strengths  $s$ . Each column from left to right in turn indicates the different

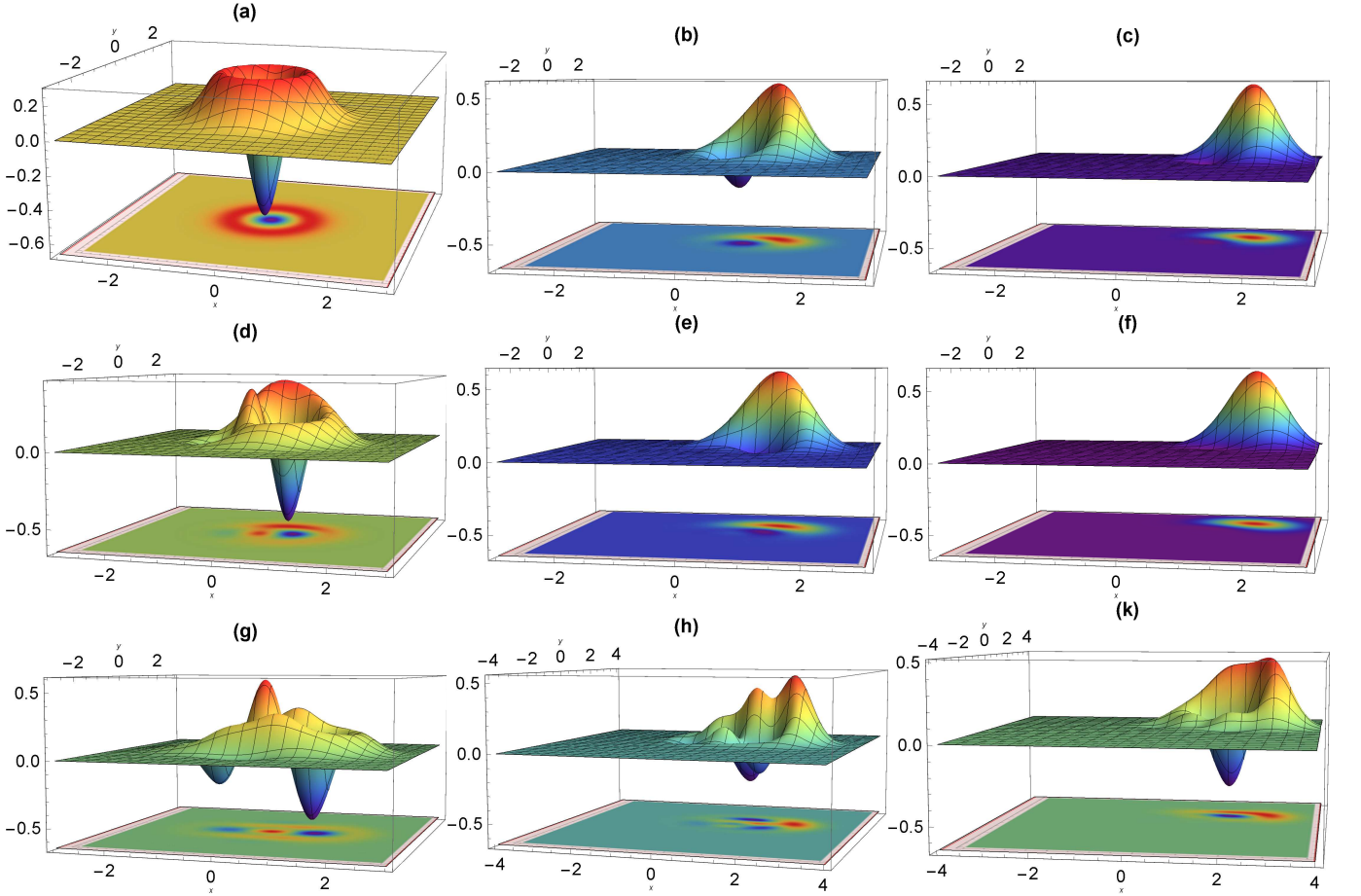


Figure 4. (Color online) Wigner function of SPACS with changing related parameters. Each column is defined for the different coherent state parameter  $\alpha$  with  $r = 0, 1, 2$ , and are ordered accordingly from left to right. Figures (a) to (c) correspond to  $s = 0$ , (d) to (f) correspond to  $s = 0.5$ , and (g) to (k) correspond to  $s = 2$ , respectively. Other parameters are the same as Fig. (3).

coherent state parameters  $r$  for 0, 1 and 2, and each row from up to down represents the different coupling strengths  $s$  for 0, 0.5 and 2, respectively. It is observed that the positive peak of the Wigner function moves from the center to the edge position in phase space and its shapes gradually became irregular with changing the coupling strength  $s$ . From the first row (see the Figs. 4(a-c)) we can see that the original SPACS shows its inherent features changed from single photon state to coherent states with gradually increasing the coherent state parameter  $r$ . Figs. 4(d-k) indicates the phase space density function  $W(z)$  after postselected von Neumann measurement. Fig. 4 (d-f) represents the Wigner function for fixed weak interaction strength  $s = 0.5$ , it can be observed that the Wigner function distribution shows

squeezing in phase space compared to the original SPACS and this kind of squeezing is pronounced with the increasing the coupling strength (see the Figs. 4(g-k)). Furthermore, in Figs. 4(g-k) we can see that in strong measurement regime the significant interference structures are occurred and the negative regions also become larger than initial pointer state.

As mentioned above, the existence and the area of negative parts of the Wigner function in phase space indicates the degree of nonclassicality of the associated state. From the above analysis we can conclude that after the postselected von Neumann measurement the phase space distribution of SPACS not only squeezed but also the nonclassicality pronounced in strong measurement regime.

## V. CONCLUSION

In this paper we have studied the squeezing and Wigner function of SPACS after postselected von Neu-

mann measurement. In order to achieve our goal, first of all we get the final state of the pointer state along with the standard measurement process. We examined the or-

binary (first-order) and ASS effects after measurement, and found that in the weak measurement region, the ordinary squeezing and ASS of the light field increased significantly as the weak value increases.

To further explain our work, we examined the similarity between the initial SPACS and the state after measurement. We observed that in the weak coupling, the state after post-selected measurement is keep its similarity with initial state. However, as the intensity of the measurement increases, the similarity between them gradually decreased and indicated that the measurement spoiled system state if the it is a strong measurement. We also investigate the Wigner function of the system after postselected measurement. It is observed that following with the postselected von Neumann measurement, the phase space distribution of SPACS is not only squeezed, but also undergoes a significant interfer-

ence structures in the strongly measured regime, meanwhile it possess pronounced nonclassicality characterized with large negative area in phase space.

We anticipate that the theoretical scheme in this paper could provide some effective methods for practical problems in quantum information processing associated with the SPACS.

## ACKNOWLEDGMENTS

This work was supported by the Natural Science Foundation of Xinjiang Uyghur Autonomous Region (Grant No. 2020D01A72), the National Natural Science Foundation of China (Grant No. 11865017) and the Introduction Program of High Level Talents of Xinjiang Ministry of Science.

---

[1] A. Mari and J. Eisert, *Phys. Rev. Lett.* **103**, 213603 (2009).  
[2] Y. Yamamoto and H. A. Haus, *Rev. Mod. Phys.* **58**, 1001 (1986).  
[3] H. Yuen and J. Shapiro, *IEEE. T. Inform. Theory* **26**, 78 (1980).  
[4] S. L. Braunstein and H. J. Kimble, *Phys. Rev. Lett.* **80**, 869 (1998).  
[5] R. Lo Franco, G. Compagno, A. Messina, and A. Napoli, *Phys. Rev. A* **76**, 011804 (2007).  
[6] R. L. Franco, G. Compagno, A. Messina, and A. Napoli, *Int. J. Quantum. Inf* **07**, 155 (2009).  
[7] R. L. Franco, G. Compagno, A. Messina, and A. Napoli, *Open. Syst. Inf. Dyn* **13**, 463 (2006).  
[8] R. Lo Franco, G. Compagno, A. Messina, and A. Napoli, *Phys. Rev. A* **74**, 045803 (2006).  
[9] R. Lo Franco, G. Compagno, A. Messina, and A. Napoli, *Eur. Phys. J-Spec. Top* **160**, 247 (2008).  
[10] R. Lo Franco, G. Compagno, A. Messina, and A. Napoli, *Phys. Lett. A* **374**, 2235 (2010).  
[11] B. R. Mollow and R. J. Glauber, *Phys. Rev.* **160**, 1076 (1967).  
[12] R. Slusher and B. Yurke, *J. Lightwave. Technol* **8**, 466 (1990).  
[13] H. Yuen and J. Shapiro, *IEEE. T. Inform. Theory* **24**, 657 (1978).  
[14] C. M. Caves, *Phys. Rev. D* **23**, 1693 (1981).  
[15] G. J. Milburn and S. L. Braunstein, *Phys. Rev. A* **60**, 937 (1999).  
[16] B. Schumacher, *Phys. Rev. A* **54**, 2614 (1996).  
[17] B. Schumacher and M. A. Nielsen, *Phys. Rev. A* **54**, 2629 (1996).  
[18] F.-l. Li, H.-r. Li, J.-x. Zhang, and S.-y. Zhu, *Phys. Rev. A* **66**, 024302 (2002).  
[19] T. C. Zhang, K. W. Goh, C. W. Chou, P. Lodahl, and H. J. Kimble, *Phys. Rev. A* **67**, 033802 (2003).  
[20] B. Kraus, K. Hammerer, G. Giedke, and J. I. Cirac, *Phys. Rev. A* **67**, 042314 (2003).  
[21] A. Kitagawa and K. Yamamoto, *Phys. Rev. A* **68**, 042324 (2003).  
[22] A. Dolińska, B. C. Buchler, W. P. Bowen, T. C. Ralph, and P. K. Lam, *Phys. Rev. A* **68**, 052308 (2003).  
[23] S. L. Braunstein and H. J. Kimble, *Phys. Rev. A* **61**, 042302 (2000).  
[24] V. Petersen, L. B. Madsen, and K. Mølmer, *Phys. Rev. A* **72**, 053812 (2005).  
[25] J. Kempe, *Phys. Rev. A* **60**, 910 (1999).  
[26] C. K. Hong and L. Mandel, *Phys. Rev. A* **32**, 974 (1985).  
[27] M. Hillery, *Opt. Commun* **62**, 135 (1987).  
[28] M. Hillery, *Phys. Rev. A* **36**, 3796 (1987).  
[29] C. Gerry and S. Rodrigues, *Phys. Rev. A* **35**, 4440 (1987).  
[30] Xiaoping Yang and Xiping Zheng, *Phys. Lett. A* **138**, 409 (1989).  
[31] E. K. Bashkirov and A. S. Shumovsky, *Int. J. Mod. Phys. B* **4**, 1579 (1990).  
[32] M. H. Mahran, *Phys. Rev. A* **42**, 4199 (1990).  
[33] P. Marian, *Phys. Rev. A* **44**, 3325 (1991).  
[34] M. A. Mir, *Int. Journ. Mod. Phys. B* **7**, 4439 (1993).  
[35] S.-d. Du and C.-d. Gong, *Phys. Rev. A* **48**, 2198 (1993).  
[36] A. V. Chizhov, J. W. Haus, and K. C. Yeong, *Phys. Rev. A* **52**, 1698 (1995).  
[37] R. Lynch and H. A. Mavromatis, *Phys. Rev. A* **52**, 55 (1995).  
[38] M. A. Mir, *Int. J. Mod. Phys. B* **12**, 2743 (1998).  
[39] R.-H. Xie and S. Yu, *J. Opt. B-Quantum. S. O* **4**, 172 (2002).  
[40] R.-H. Xie and Q. Rao, *Physica. A* **312**, 421 (2002).  
[41] Z. Wu, Z. Cheng, Y. Zhang, and Z. Cheng, *Physica. B* **390**, 250 (2007).  
[42] E. K. BASHKIROV, *Int.J. Mod. Phys.B* **21**, 145 (2007).  
[43] D. K. Mishra, *Opt. Commun* **283**, 3284 (2010).  
[44] D. K. Mishra and V. Singh, *Opt. Quant. Electron* **52**, 68 (2020).  
[45] S. Kumar and D. K. Giri, *J. Optics-UK* **49**, 549 (2020).  
[46] Y. Wang, W.-S. Bao, H.-Z. Bao, C. Zhou, M.-S. Jiang, and H.-W. Li, *Phys. Lett. A* **381**, 1393 (2017).  
[47] M. Miranda and D. Mundarain, *Quant. Infor. Proc* **16**, 298 (2017).  
[48] J.-J. Chen, C.-H. Zhang, J.-M. Chen, C.-M. Zhang, and Q. Wang, *Quant. Infor. Proc* **19**, 198 (2020).  
[49] Y. Aharonov, D. Z. Albert, and L. Vaidman, *Phys. Rev. Lett.* **60**, 1351 (1988).

[50] K. Nakamura, A. Nishizawa, and M.-K. Fujimoto, *Phys. Rev. A* **85**, 012113 (2012).

[51] B. de Lima Bernardo, S. Azevedo, and A. Rosas, *Opt. Commun.* **331**, 194 (2014).

[52] Y. Turek, H. Kobayashi, T. Akutsu, C.-P. Sun, and Y. Shikano, *New. J. Phys* **17**, 083029 (2015).

[53] Y. Turek, W. Maimaiti, Y. Shikano, C.-P. Sun, and M. Al-Amri, *Phys. Rev. A* **92**, 022109 (2015).

[54] Y. Turek and T. Yusufu, *Eur. Phys. J. D* **72**, 202 (2018).

[55] Y. Turek, *Chin. Phys. B* **29**, 090302 (2020).

[56] Y. Turek, *Eur. Phys. J. Plus* **136**, 221 (2021).

[57] von Neumann J, *Mathematical Foundations of Quantum Mechanics* (Princeton University Press, Princeton, NJ, 1955).

[58] Y. Aharonov and A. Botero, *Phys. Rev. A* **72**, 052111 (2005).

[59] A. Di Lorenzo and J. C. Egues, *Phys. Rev. A* **77**, 042108 (2008).

[60] A. K. Pan and A. Matzkin, *Phys. Rev. A* **85**, 022122 (2012).

[61] G. Agarwal, *Quantum Optics* (Cambridge University Press, Cambridge, England, 2013).

[62] P. Shukla and R. Prakash, *Mod. Phys. Lett. B* **27**, 1350086 (2013).